Dalton Transactions

ARTICLE

The folding of a metallopeptide

Ilaria Gamba,[a] Gustavo Rama,[a] Elisabeth Ortega-Carrasco,[b] Roberto Berardozzi,[c] Víctor M. Sánchez-Pedregal,[d] Lorenzo Di Bari,[c] Jean-Didier Maréchal,*[,b] M. Eugenio Vázquez,*[,d] Miguel Vázquez López*[,a]

Received 00th January 20xx,
Accepted 00th January 20xx

DOI: 10.1039/x0xx00000x

www.rsc.org/

We have applied solid-phase synthesis methods for the construction of tris(bipyridyl) peptidic ligands that coordinate Fe(II) ions with high affinity and fold into stable mononuclear metallopeptides. The main factors influencing the folding pathway and chiral control of the peptidic ligands around the metal ions has been studied both by experimental techniques (CD, UV-vis and NMR) and molecular modeling tools. Amongst the numerous molecular variables that have been studied, this study clearly illustrates how the chirality of a given set of aminoacids (proline in this case) of the peptide dictates the chirality of the metal center of the resulting metallopeptide. Moreover, the reatively hydrophobic peptidic models used in this work show that the most stable structures present reduced solvent contacts and, in couterpart, stabilize *cis* configuration of the proline residues.

Introduction

Understanding the way in which peptides and proteins fold into functional architectures in an autonomously-guided mechanism defined by the amino acid sequence, that is, the protein folding problem, has been a formidable scientific challenge since its identification more than 50 years ago. [1,2] Moreover, despite the increasing success in the prediction of the three dimensional structures of small proteins and peptides,[3] the study of metallopeptides—how they fold and misfold,[4] aggregate,[5] or interact with other molecules—is still in its infancy.[6,7] These studies are of great relevance, given the role of metal ions in the folding/misfolding of metalloproteins and also in relevant pathological processes, such as the induction of amyloid aggregation and precipitation in neurodegenerative diseases.[8] One of the main reasons for this underdevelopment is that the breakdown of the different energies involved in the folding of metallopeptides is very difficult to establish with peptides coded by the 20 natural amino acids, because too many physicochemical variables are involved when the donor atoms suitable for coordination are located in the side chains of the peptide sequence. In contrast, artificial metallopeptides, in which the metal-binding units are part of the main chain of the amino acid structure, represent excellent model systems for the study of metallopeptide folding, as they can be described with far less variables and offer much better coupling between the conformational preferences of the peptide chain and the coordinating properties of the metal ions.[9,10,11] Herein, we present a computational and experimental study of the folding and chiral control of a family of octahedral mononuclear metallopeptides containing metal-coordinating bipyridyl units as integral part of the peptide backbone, and describe important factors that influence the metal-directed folding of the peptide ligands into chiral structures.

Results and discussion

2,2'-bipyridine (Bpy) is a privileged metal chelator and, as such, has been extensively used in coordination and supramolecular chemistry.[12] We synthesized a Bpy analog appropriately modified for its application in solid phase peptide synthesis (SPPS) in which the Bpy unit was derivatized as a Fmoc-protected amino acid with 5-amino-3-oxapentanoic acid (Fmoc-O1PenBpy-OH, **1**, Scheme 1). Following the synthesis of the amino acid building block, we designed a set of six peptide ligands featuring three metal-binding bipyridine units connected by two short loops (**LL-P**, **DD-P**, **GD-P**, **GL-P**, **DL-P** and **LD-P**, Scheme1). The loops include a *β*-turn promoting sequence (Pro-Gly) that directs the folding of the peptide

[a] Departamento de Química Inorgánica and Centro Singular de Investigación en Química Biolóxica e Materiais Moleculares (CiQUS). Universidade de Santiago de Compostela, 15782 Santiago de Compostela, Spain. E-mail: miguel.vazquez.lopez@usc.es.
[b] Departament de Química. Universitat Autònoma de Barcelona, 08193 Cerdanyola, Spain E-mail: jeandidier.marechal@uab.cat.
[c] Dipartimento di Chimica e Chimica Industriale. Università di Pisa. 56124 Pisa, Italy.
[d] Departamento de Química Orgánica and Centro Singular de Investigación en Química Biolóxica e Materiais Moleculares (CiQUS). Universidade de Santiago de Compostela 15782 Santiago de Compostela, Spain. E-mail: eugenio.vazquez@usc.es.

Electronic Supplementary Information (ESI) available: [Synthesis and characterization of the coordinating residue, ligand peptides and metallopeptides; details and further data about the NMR, CD and UV-vis studies; details and further data about the molecular modelling and CD/DFT studies]. See DOI: 10.1039/c000000x/

chains into discrete mononuclear species and encodes the chirality of their resulting complexes; [9] the N-terminal loop may contain a chiral proline (–Gly-(L)Pro-Gly– or –Gly-(D)Pro-Gly–), or an achiral sequence (–Gly-Gly-Gly–), while the C-terminal loop contains in all cases a chiral proline residue (–Gly-(L)Pro-Gly– or –Gly-(D)Pro-Gly–). All the peptides were obtained using standard Fmoc/tBu solid-phase protocols,[13] and the final products were purified by reverse-phase HPLC and identified by MS (see ESI).

Following the synthesis of the peptide ligands, we first studied the thermodynamic stability of their metal complexes. Thus, incubation of low μM solutions of the peptide ligands **LL-P** (featuring homochiral Pro loops), **GL-P** (one chiral loop), and **DL-P** (heterochiral loops) at 298 K with Fe(II) ions resulted in qualitatively similar changes, most notably a clear bathochromic shift of the Bpy absorption band from 308 to approximately 316 nm due to the complexation processes (See ESI, Figures S1-S3). The binding constants derived from the UV/vis titrations indicate that all the complexes are very stable, so that the values of the formation constants are $\beta_{1,1} \approx 8$ for **LL-P** and **GL-P**, and $\beta_{1,1} \approx 9$ for the more stable heterochiral peptide complex with **DL-P** (ESI, Figures S4-6 and Table S1).[14] The assembly of the discrete mononuclear octahedral complexes was further confirmed by MALDI-TOF mass spectrometry (See ESI).[15]

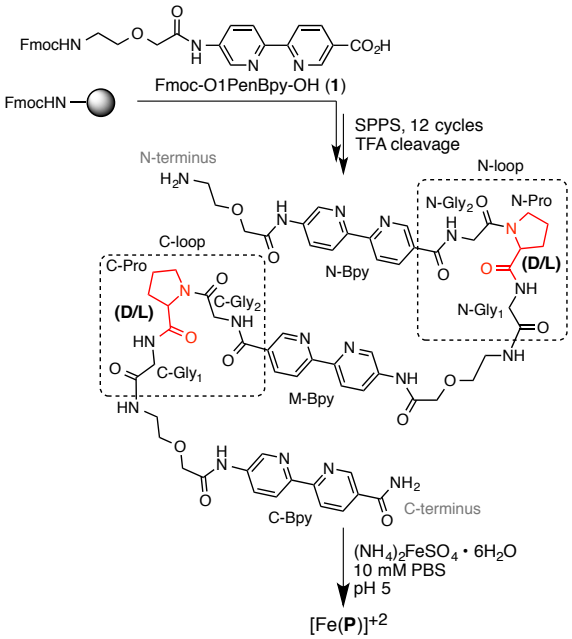

	N-loop	C-loop
LL-P:	–Gly–(L)Pro–Gly–	–Gly–(L)Pro–Gly–
DD-P:	–Gly–(D)Pro–Gly–	–Gly–(D)Pro–Gly–
LD-P:	–Gly–(L)Pro–Gly–	–Gly–(D)Pro–Gly–
DL-P:	–Gly–(D)Pro–Gly–	–Gly–(L)Pro–Gly–
GL-P:	–Gly–Gly–Gly–	–Gly–(L)Pro–Gly–
GD-P:	–Gly–Gly–Gly–	–Gly–(D)Pro–Gly–

Scheme 1. Solid phase peptide synthesis of the tris(bipyridyl) peptide ligands **LL-P**, **DD-P**, **LD-P**, **DL-P**, **GL-P** and **GD-P**, as well as their corresponding Fe(II) mononuclear octahedral complexes.

As expected, the enantiomeric **LL-P** and **DD-P** ligands give rise to mirror image CD spectra characterized by two bands of opposite sign at 300 and 329 nm with a crossover at 314 nm, so that **LL-P** displays a positive couplet and **DD-P** a negative couplet. It is worth recalling that a CD couplet is defined a sequence of two bands of approximately equal amplitude and opposite signs, with crossover point close to the absorption maximum; the couplet is defined positive/negative according to the sign of its long-wavelength component. The intensity of these bands increases upon addition of 1 equivalent of Fe(II) ions and their increase is also accompanied by bathochromic shifts of both couplet components, respectively. Furthermore, upon iron chelation we observe the appearance of another broad bisignate feature allied to a charge transfer transitions around 550 nm. As observed in other cases before, this pair of bands in the *vis*-region have opposite sign sequence with respect to the UV-couplet.[16] The sign of the UV-couplet is consistent with a Λ configuration in the metal centre for [Fe(**LL-P**)]$^{2+}$ and with the opposite Δ configuration for [Fe(**DD-P**)]$^{2+}$ (Figure 1).[17] Interestingly, the CD spectra of the **LL-P**, **LD-P** and **DD-P** systems indicate that a single Pro residue in the sequence (namely, the N-terminal Pro) encodes the dominating chirality of the resulting metallopeptide. Thus, the CD spectra of **LD-P** and **LL-P**, as well as those of their corresponding Fe(II) complexes, [Fe(**LD-P**)]$^{2+}$ and [Fe(**LL-P**)]$^{2+}$ display a positive UV-couplet around 300 nm, and correspondingly a negative/positive sequence long-wavelength bands around 550 (Figure 1 and ESI, Figures S7-9). The presence of the UV couplet before complexation and the conservation of its sign (although with a significant increase in amplitude) after metal binding suggests that the bipyridyl moieties in the free peptides are to some extent preorganized to host the metal.

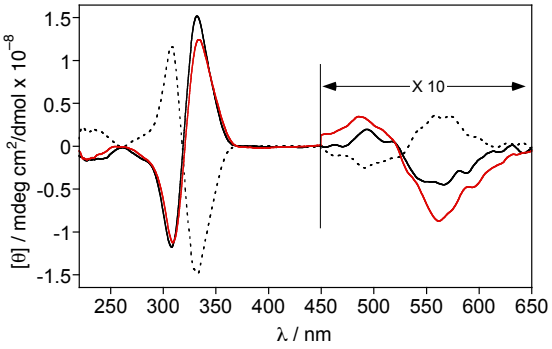

Figure 1. a) CD spectra of [Fe(**LL-P**)]$^{2+}$ (black line), [Fe(**LD-P**)]$^{2+}$ (red line), and [Fe(**DD-P**)]$^{2+}$ (dashed line). CD spectra were measured at 293 K, 10 mM PBS buffer, pH = 5.0.

While conducting these CD studies we became aware that the assembly of the Fe(II) metallopeptides is a kinetically slow process, and therefore we decided to monitor the folding of the peptide ligands in presence of Fe(II) ions. The homochiral ligands (**LL-P** and **DD-P**) displayed a monoexponential decrease (or increase) of their 332 nm CD signal at 40 ºC upon addition of Fe(II), reaching a plateau after approximately 25 min (Figure 2a), consistent with a two-state process in which the unfolded

peptides reach thermodynamic equilibrium as folded Fe(II)-metallopeptides (*U* ⇄ *F*). The simple two-state process is also confirmed by the existence of a isodichroic point.[18] In contrast with this, the intensity of the CD signal at 332 nm of the peptides containing two proline residues with opposite chirality (**DL-P** and **LD-P**) displays a biphasic profile at 40 ºC, and lacks the isodichroic point, so that a rapid increase (or decrease) in the CD intensity is followed by a slower exponential decay (or increase) (Figure 2b). In this case, the folding process cannot be simply described by the direct transition between an unfolded and a folded state (*U* ⇄ *F*), but requires the consideration of an intermediate complex (*U* ⇄ *I* ⇄ *F*). Moreover, lowering the temperature from 40 ºC to 20 ºC resulted in an increase of the CD signal, but more importantly, it also induced a change in the kinetic profiles of the homochiral peptides, which become biphasic at 20 ºC, thus suggesting the accumulation at this temperature of an intermediate complex similar to that observed for the mixed chirality peptides also at higher temperatures. In contrast with this, the mixed chirality peptide, **DL-P** as well as those with a single Pro residue, **GL-P** and **GD-P**, maintain their folding profiles, albeit with at significantly slower rate (see ESI for the kinetic constants, Table S2).

In all cases the observed changes in the CD only affect the intensity of the bands, but not their position, and these variations are not observed in the absorption spectra (ESI, Figures S13-21). This suggests that the variations in the CD intensity arise from changes in the relative position of the Bpy chromophores around the metal center as they rearrange to their most stable geometry through non-dissociative mechanisms, such as the Bailar or the Ray–Dutt twists isomerizations.[19]

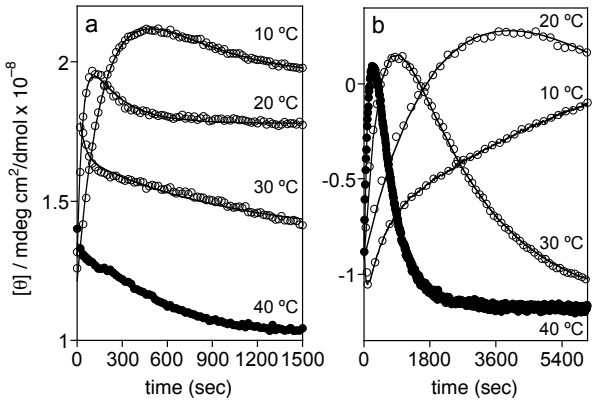

Figure 2. Evolution of the circular dichroism signal at 332 nm of **LL-P** (a), and **DL-P** (b) upon addition of Fe(II) at various temperatures. **LL-P** Shows monoexponential decays at 40 and 30 ºC, and the biphasic profiles only appear at lower temperatures. **DL-P** shows slower kinetics (note the timescale of the plots) with biphasic profiles at all temperatures.

At this point, we decided to further investigate the folding process of the metallopeptide assembly by experimental and theoretical tools. Surprisingly, HPLC analysis of the **DL-P** heterochiral peptide ligand in the presence of Fe(II) ions shows four peaks (ESI, Figure S22), suggesting the presence of four major isomers in solution. Moreover, these four complexes are in equilibrium, as evidenced by the observation of the same four peaks when each of the isolated peaks is injected back into the HPLC after a short equilibration time. **LL-P** and **GL-P** Fe(II) metallopeptides also show the same behaviour. Moreover, the solution ^{1}H-NMR spectrum of [Fe(**LL-P**)]$^{2+}$ shows a set of resonances compatible with four distinct isomers (ESI, Figures S23-28). We tried to assess whether these isomers are in chemical exchange equilibrium by variable temperature NMR in the 5-45 ºC range (ESI, Figure S29), but no sign of chemical exchange was evident in this range. This is compatible with a slow rate of interconversion between the four isomers at the NMR timescale in the thermodynamic equilibrium suggested by the observations made by HPLC.

Molecular modeling and QM/MM optimization provided 3D models of the possible Fe(II) isomers derived from the **DL-P** ligand. These studies show that several (10) isomeric metallopeptide configurations differing in the folding of the peptidic chain around the metal center are energetically accessible (Figure 3 and ESI, Figures S30). It is worth noting that the lowest energy structure contain two *cis* prolines which suggests that during the metallopeptide assembly process these residues isomerize from their more stable *trans* conformation in solution[20] to satisfy the conformational requirements for metal coordination (see ESI Figure S31-33).[21] The energetic breakdown of the total QM/MM energy does not show major constraints on the first coordination sphere of the Fe(II) ion, and the fold of the rest of the peptide is mainly function of the energy of the loops (see ESI Figure S34). However, when considering the complete set of physical variables taken into account in our calculations, we observe that the major factor influencing the relative stability of the different isomers is the desolvation of the peptide chain that favors the more compact structures.[22]

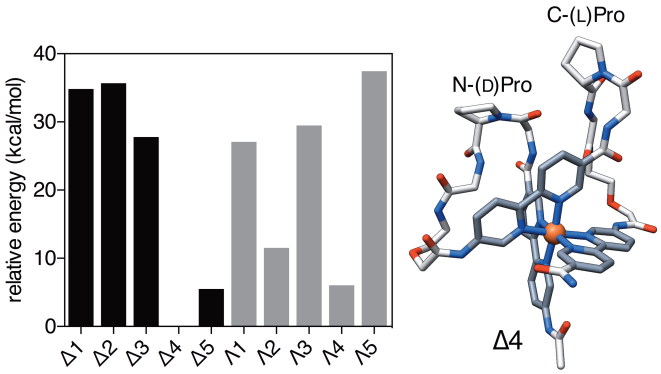

Figure 3. Left, QM/MM relative energies of the possible Fe(II) complexes formed with the **DL-P** peptide ligand. Δ isomers are shown in black and Λ in light grey. The [Fe(**DL-P**)]$^{2+}$ isomer labelled as Δ4, which has the lowest energy of all the complexes, is represented on the right (bipyridines in darker shade of grey). Please see Fig. S37 in order to compare this *cis*-Pro isomer with a trans-Pro **DL-P** analogue.

As we have seen, the CD spectra of the final mixtures of four isomers (Figure 1 and ESI, Figures S7-9) indicate an overall chiral selection governed by the chirality of the N-terminal Pro residue. Computation on the six metallopeptide systems (**LL-P/DD-P**, **GD-P/GL-P**, **DL-P/LD-P**) are not entirely conclusive regarding the fact that the overall chirality of the systems is independent of the chirality of the Pro residue in the C-terminal loop (ESI, Figures S31-33). Indeed, Δ4 and Λ4 structures are always close in energy in the six systems, despite presenting opposite chirality. We therefore look for a possible dynamical reason of the N-terminal importance in defining the chirality of the final species. Because the relative position of the Pro residues to the terminal bipyridine groups could be responsible of a difference in their flexibility, we hypothesized that it could lead to major preorganization for metal binding at the N-terminal end. An additional set of calculations was therefore performed with a 1ns MD of **DD-P** and **LL-P** isolated ligands. The analysis of the MD shows that the C-terminal Bpy unit (C-Bpy) is more flexible, and conformationally less defined than the N-Bpy group (Scheme 1), and also that the N-Bpy/M-Bpy pair is more preorganized than the M-Bpy/C-Bpy (ESI, Figure S35 and S36).

The ECD spectra for the 10 structures discussed above for the **LD-P** system (Figure 3; ESI, Figures S38-41) were simulated by means of time dependent DFT calculations (TD-DFT). To this end, we pruned the chromophores by replacing the chains at the sides of the amide groups with H-atoms. All the hydrogen atoms were reoptimized with standard DFT (CAM-B3LYP//SVP), clamping all the remaining atoms in their original positions. This truncation simplified the calculations, which otherwise would be excessively demanding, and it was justified by the fact that the chains connecting the bipyridyl amides provide only weak spectroscopic contributions. TDDFT at the same level used for geometry optimizations (CAM-B3LYP/SVP) provided the ECD spectra for the individual conformations shown in Figures S39 and S40. The proximity and dissymmetric orientation of the three chromophores is responsible for the typical exciton couplet structure, with D and L forms yielding positive and negative couplets, respectively.

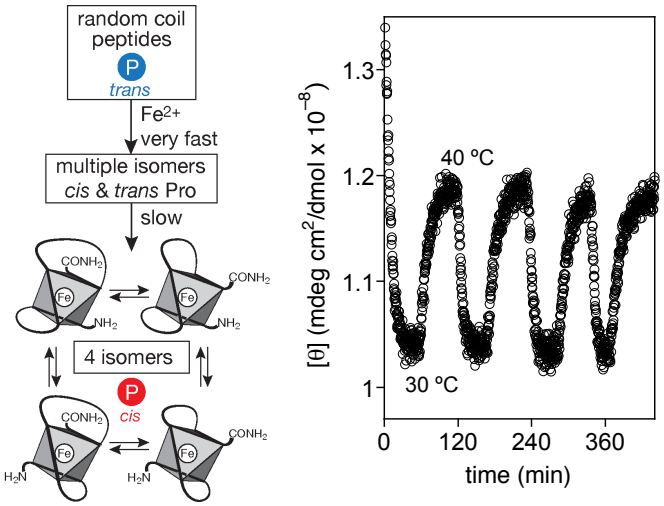

Figure 4. Left: Proposed complexation/folding mechanism of the metallopeptides involving initial coordination to the peptide ligands predominantly in *trans*-Pro configurations, and subsequent rearrangement and selection under thermodynamic control. Right: Circular dichroism of a 110 μM solution of $[Fe(\textbf{LL-P})]^{2+}$ in 10 mM phosphate buffer pH 5.0 showing the reversible modification of the CD signal (332 nm) in response to changes in the temperature (30-40ºC).

These theoretical predictions could be useful to explain the observations made during the CD *vs* time experiments above described. In fact, the timescale of the kinetic profiles suggests that the *trans* → *cis* isomerization of the proline residues is the underlying process promoting the reorganization of the peptide ligands around the metal ions.[23] This is in agreement with the known preference of Pro residues to present a *trans* conformation in short peptides in solution,[20] and the molecular modelling studies showing that the M-Bpy/N-Bpy pair is significantly structured (and thus stabilizing an otherwise unstable *cis* proline in the N-loop). Moreover, Pro isomerization has also been proposed as the slow step in the denaturation/folding pathway of small proteins.[24] The folding of these Fe(II) trisbipyridyl metallopeptides could be explained as follows (Figure 4, left). In the initial state the free peptide ligands are poorly structured (particularly their C-terminal end), and have their Pro residues in *trans* configuration; the addition of Fe(II) ions to the solution of the peptide ligands gives rise to a number of isomeric metallopeptides in equilibrium, which progressively collapse into the observed set of four isomers, which may have their Pro residues in the *cis* conformation. Interestingly, the position of the equilibrium between the selected isomers can be shifted by changes in the temperature. Thus for example, varying the temperature of a $[Fe(\textbf{LL-P})]^{2+}$ solution between 30 and 40 ºC results in measurable changes in the CD spectrum, which can be reversibly switched between two extreme values (Figure 4, right). Given the conformational manifold described above, the reversibility displayed in this variable temperature experiment is remarkable. Moreover, this figure reveals another important aspect: it describes the amplitude of a CD band due to exciton coupling of the bipyridyl groups. In a simple picture, where at higher temperature corresponds looser structures, one would expect that this amplitude should diminish, which is exactly opposite to the experimental finding. This demonstrates that between 30° and 40° C there occurs a relative population shift between two stable conformations and not just a process of melting of secondary structure.

Conclusions

In summary, we describe the folding process of a family of trisbipyridyl Fe(II) mononuclear metallopeptides. The two-step folding process involves a rapid coordination of the ligand peptides to the Fe(II) ions and the formation of a number of isomers (up to 10 possible species can be formed); this mixture collapses into four well-defined isomers. Based on high-level theoretical calculations and kinetic data, we suggest that the key factor that drives the folding pathway is a trans → cis

isomerization of the Pro residues located in the loops of the peptides connecting the three coordinating bipyridine units. Moreover, we have also observed that the position of the equilibrium between the four isomers can be reversibility switched by varying the temperature of the solution mixture. Finally, we have shown that there is an overall chiral selection in the mixture of isomers in the equilibrium, and that it is programmed by the chirality of the N-terminal Pro residue in the peptide ligand. We believe that these studies could help to improve the scarce knowledge about the folding mechanism in metallopeptides and metalloproteins.

Acknowledgements

We are thankful for the support given by the Spanish grants SAF2013-41943-R, CTQ2012-31341, CTQ2011-23336 and CTQ2013-49317-EXP; the ERDF and the European Research Council (Advanced Grant 340055); the Xunta de Galicia grants GRC2013-041 and PGIDIT08CSA-047209PR and the Generalitat de Catalunya grant 2009SGR68. Support of COST Action CM1105 is kindly acknowledged. G.R. thanks the INL for his PhD fellowship.

Notes and references

1 J. C. Kendrew, G. Bodo, H. M. Dintzis, R. G. Parrish and H. Wyckoff, *Nature*, 1958, **181**, 662–666.

2 C. B. Anfisen, *Science*, 1973, **181**, 223–230; b) K. A. Dill and J. L. MacCallum, *Science*, 2012, **338**, 1042–1046.

3 R. Schweitzer-Stenner, V. Uversky. *Peptide Folding, Misfolding & Nonfolding* (Ed.: R. Schweitzer-Stenner). Wiley-VCH. 2012.

4 D. Shortle, *FASEB J.,* 1996, **10**, 27–34.

5 A. Aguzzi and T. O'Connor, *Nat. Rev. Drug. Discov*., 2010, **9**, 237–248.

6 V. Lykourinou, L.-J. Ming in *Metallofoldamers: Supramolecular Architectures from Helicates to Biomimetics* (Eds.: G. Maayan, M. Albrecth), Wiley-VCH, 2013, pp. 1–50.

7 E. Ortega-Carrasco, A. Lledós, J.-D. Maréchal, *J. R. Soc. Interface*, 2014, **11**, 20140090

8 a) E. House, J. Collingwood, A. Khan, O. Korchazkina, G. Berthon and C. Exley, *J. Alzheimers Dis.,* 2004, **6**, 291–201; b) C. Exley, *J. Alzheimers Dis.*, 2006, **10**, 173–177; c) E. Permyakov, *Metallloproteomics*, John Wiley & Sons, Hoboken, New Jersey (USA), 2009.

9 G. Rama, A. Ardá, J.-D. Maréchal, I. Gamba, H. Ishida, J. Jiménez-Barbero, M. E. Vázquez and M. Vázquez López, *Chem. Eur. J.,* 2012, **18**, 7030–7035.

10 I. Gamba, I. Salvadó, G. Rama, M. Bertazzon, M. I. Sánchez, V. M. Sánchez-Pedregal, J. Martínez-Costas, R. F. Brissos, P. Gamez, J. L. Mascareñas, M. Vázquez López and M. E. Vázquez, *Chem. Eur. J*., 2013, **19**, 13369–13375.

11 I. Gamba, G. Rama, E. Ortega-Carrasco, J.-D. Maréchal, J. Martínez-Costas, M. E. Vázquez and M. Vázquez López, *Chem. Commun*., 2014, **50**, 11097–11100.

12 C. Kaes, A. Katz and M. W. Hossein, *Chem. Rev.* 2000, **100**, 3553.

13 I. Coin, M. Beyermann and M. Bienert, *Nature Prot*., 2007, **2**, 3247.

14 The best fit to the experimental data suggests a significant proportion of the 1:2 ML species in the initial steps of the UV-vis titrations, when the peptidic ligand is in greater excess over the metal ion. Further increase in the metal-to-ligand ratios, progressively shifts the equilibrium towards the expected 1:1 complex later in the titration.

15 The UV-vis spectra of the Fe(II) metallopeptides show intense bands centered at 543 nm. These data, together with the MALDI spectra, suggest octahedral coordination geometries of the metal centers in their respective complexes.

16 J. Dragna, G. Pescitelli, L. Tran, V. M. Lynch, E.V. Anslyn, L. Di Bari, *J. Am. Chem. Soc.,* 2012, **134**, 4398-4407.

17 a) H. Mürner, P. Belser and A. Zelewsky, *J. Am. Chem. Soc*., 1996, **118**, 7989–7994; b) P. Wang, J. E. Miller, L. M. Henling, C. L. Stern, N. L. Frank, A. L. Eckerman and T. J. Meade, *Inorg. Chem*., 2007, **46**, 9853–9862.

18 G. Pescitelli, L. Di Bari, N. Berova, *Chem. Soc. Rev*., 2013, **43**, 5211-5233.

19 A. Rodger and B. F. G. Johnson, *Inorg. Chem.,* 1988, **27**, 3061–3062; M. Amati and F. Lelj, *Theor. Chem. Account*, 2008, **120**, 447–457.

20 a) J. Brandts, H. Halvorson and M. Brennan, *Biochemistry*, 1975, **14**, 4953-4963; b) C. Dugave and L. Demange, *Chem. Rev.*, 2003, **103**, 2475-2532.

21 J. F. Brandts, H. R. Halvorson and M. Brennan, *Biochemistry*, 1975, **14**, 4953–4963.

22 O. Bignucolo, H. T. Leung, S. Grzesiek and S. Bernèche, *J. Am. Chem. Soc.,* 2015, **137,** 4300–4303.

23 a) W. A. Thomas and M. K. Williams, *J. Chem. Soc., Chem. Commun.,* 1972, 994; b) D. Kern, M. Schutkowski and T. Drakenberg, *J. Am. Chem. Soc.,* 1997, **119,** 8403–8408.

24 J. F. Brandts, H. R. Halvorson and M. Brennan, *Biochemistry,* 1975, **14,** 4953–4963.